Received: 24 September 2019 | Revised: 27 December 2019 | Accepted: 27 December 2019

DOI: 10.1096/fj.201902391R

RESEARCH ARTICLE

THE FASEB JOURNAL

S1P d20:1, an endogenous modulator of S1P d18:1/S1P$_2$-dependent signaling

Rajkumar Vutukuri[1] | Alexander Koch[1] | Sandra Trautmann[2] | Yannick Schreiber[3] | Dominique Thomas[2] | Franziska Mayser[4] | Dagmar Meyer zu Heringdorf[1] | Josef Pfeilschifter[1] | Waltraud Pfeilschifter[4] | Robert Brunkhorst[4]

[1]Institute of General Pharmacology and Toxicology, University Hospital, Goethe University Frankfurt, Frankfurt am Main, Germany

[2]Institute of Clinical Pharmacology, University Hospital, Goethe University Frankfurt, Frankfurt am Main, Germany

[3]Fraunhofer Institute of Molecular Biology and Applied Ecology-Project Group Translational Medicine and Pharmacology (IME-TMP), Frankfurt am Main, Germany

[4]Department of Neurology, University Hospital, Goethe University Frankfurt, Frankfurt am Main, Germany

Correspondence
Robert Brunkhorst, Department of Neurology, Goethe University Hospital, Frankfurt am Main, Germany.
Email: robert.brunkhorst@kgu.de

Funding information
Deutsche Forschungsgemeinschaft (DFG), Grant/Award Number: SFB1039; Fondation Leducq

Abstract

Sphingosine 1-phosphate (S1P) signaling influences numerous cell biological mechanisms such as differentiation, proliferation, survival, migration, and angiogenesis. Intriguingly, our current knowledge is based solely on the role of S1P with an 18-carbon long-chain base length, S1P d18:1. Depending on the composition of the first and rate-limiting enzyme of the sphingolipid de novo metabolism, the serine palmitoyltransferase, other chain lengths have been described in vivo. While cells are also able to produce S1P d20:1, its abundance and function remains elusive so far. Our experiments are highlighting the role of S1P d20:1 in the mouse central nervous system (CNS) and human glioblastoma. We show here that S1P d20:1 and its precursors are detectable in both healthy mouse CNS-tissue and human glioblastoma. On the functional level, we focused our work on one particular, well-characterized pathway, the induction of cyclooxygenase (COX)-2 expression via the S1P receptor 2 (S1P$_2$). Intriguingly, S1P d20:1 only fairly induces COX-2 expression and can block the S1P d18:1-induced COX-2 expression mediated via S1P$_2$ activation in the human glioblastoma cell line LN229. This data indicates that S1P d20:1 might act as an endogenous modulator of S1P signaling via a partial agonism at the S1P$_2$ receptor. While our findings might stimulate further research on the relevance of long-chain base lengths in sphingolipid signaling, the metabolism of S1P d20:1 has to be considered as an integral part of S1P signaling pathways in vivo.

KEYWORDS

brain, cyclooxygenase 2, glioblastoma cells, S1P receptors, sphingosine 1-phosphate

Abbreviations: BSA, bovine serum albumin; CHO, Chinese hamster ovarian; CNS, central nervous system; CoA, Coenzyme A; COX, cyclooxygenase; FCS, fetal calf serum; GBM, glioblastoma; LCB, long-chain sphingoid base; PBS, phosphate-buffered saline; PGE_2, prostaglandin E_2; S1P, sphingosine 1-phosphate; $S1P_{1\text{-}5}$, S1P receptor 1-5; SPT, serine palmitoyltransferase.

1 | INTRODUCTION

Sphingolipids are structural and signaling components of all living organisms, defined by a hydrophilic head group and a hydrophobic long-chain sphingoid base (LCB).[1] The metabolite sphingosine 1-phosphate (S1P) participates in a myriad of signaling cascades and performs indispensable functions like lymphocyte trafficking and endothelial cell function.[2] The exact mechanism of action of S1P depends on the local S1P concentration and on the cell-specific receptor profile. Indicating the importance of such regulative mechanisms, some effects of S1P are even opposing. For example, while S1P is crucial in the maintenance of vascular integrity,[3,4] it can also act as a proinflammatory mediator by inducing cyclooxygenase (COX)-2 expression and activity in various cell types.[5-7]

In the de novo synthesis of all sphingolipids, the highly conserved, rate-limiting enzyme serine palmitoyltransferase (SPT) catalyzes the initial condensation of different acyl-CoAs usually with the amino acid L-serine to form the precursor of sphingoid bases, 3-ketosphinganine. Although fatty acids such as myristoyl-CoA (with 14 carbon atoms [C14]) and stearoyl-CoA (C18) can form LCBs with a C16 and C20 chain length respectively, C18-LCBs generated by palmitoyl-CoA (C16) as a substrate are most abundant in eukaryotes.[8] The SPT is a complex composed of large subunits (SPTLC1 with either SPTLC2 or SPTLC3) and small subunits (SPTssa or SPTssb).[9] The acyl-CoA preference and formation of different LCBs are attributed to the discrete specificities of SPT subunits in the isoenzyme complex. In different studies, it was demonstrated that the SPTLC3 subunit favors the condensation of myristoyl-CoA, while the subunit SPTssb facilitates the use of stearoyl-CoA.[8,10]

The current data indicate a distinct functional relevance of sphingolipids with C20-LCBs: The precursor of stearyl-CoA, stearic acid, was demonstrated to alleviate thrombogenic and atherogenic risk factors in healthy males.[11] Importantly, higher levels of stearic acid were associated with a lower risk of cancer.[12-15] Moreover, higher concentrations of sphingolipids with C20-LCBs in plasma have also been shown to predict cardiovascular events.[16] In mice, Zhao et al have shown that the accumulation of C20-LCBs by SPTssb mutation leads to compromised neural and retinal functions.[17]

We propose that some of these functions could be mediated by changes in S1P signaling, as C18-LCBs will finally lead to S1P d18:1 and C20-LCBs to S1P d20:1. In this context, one recent study showed that S1P with C16- to C20-LCBs differ in their ability to activate the S1P receptors.[18] However, to our knowledge, quantitative data on the concentrations of sphingolipids with C20-LCBs in the organism are sparse and contradictory. While C20-LCBs were reported to be abundantly present in gangliosides of rabbit, horse, and bovine central nervous system cells and tissues,[19-21] only one study so far suggests high concentrations of S1P d20:1 in the rodent brain.[17] However, until now, no comprehensive data of the distribution and functional relevance of S1P d20:1 in vivo have been published.

The hypothesis of LCB-length-dependent efficacy of S1P[18] and the suspected abundance of sphingolipids with C20-LCBs in diverse tissues and especially the brain prompted us to investigate the functional relevance.

We investigated the S1P d20:1 concentration in central nervous system (CNS) tissue and performed first mechanistic studies to provide evidence for a potential (patho-)physiological relevance of S1P d20:1 which would add another layer of complexity to the regulation of S1P signaling.

2 | MATERIAL AND METHODS

2.1 | Materials

S1P d18:1 and S1P d20:1 were purchased from Avanti polar lipids (Alabaster, USA) and JTE-013 was from Cayman Chemicals (Michigan, USA).

2.2 | Cell culture and stimulation

LN229 human glioblastoma cells between 15 and 30 passages were cultured in 6-well cell culture plates and DMEM medium with 10% fetal calf serum (FCS) and 1% Pen/Strep was used as a growth medium. All media used for the cell culture and other components were acquired from Thermo Fisher Scientific (Darmstadt, Germany). After reaching confluency, cells were preincubated with serum-free medium. After 16 hours, LN229 cells were stimulated with S1P d18:1, S1P d20:1, and JTE-013 as indicated in the respective figure legends. All stimulations were performed for 2 hours time points unless mentioned otherwise. S1P (d18:1 and d20:1) was dissolved in 0.4% fatty acid-free bovine serum albumin (BSA) in phosphate-buffered saline (PBS). JTE-013 was dissolved in dimethyl sulfoxide. All control cells were treated with vehicle alone.

2.3 | Two-step polymerase chain reaction (PCR) analysis

Two-step PCR analysis was performed as described previously.[5] Briefly, 1 μg of total RNA was isolated with TRIZOL reagent (Sigma-Aldrich, Steinheim, Germany) according to the manufacturer's protocol and used for the reverse transcriptase-polymerase chain reaction (RT-PCR; RevertAid first strand cDNA synthesis kit, Thermo Fisher Scientific,

Darmstadt, Germany) utilizing random hexamer primers for amplification. Real-time PCR (TaqMan) was performed using the Applied Biosystems 7500 Fast Real-Time PCR System. Probes, primers, and the reporter dyes 6-FAM and VIC were from Thermo Fisher Scientific (Darmstadt, Germany). The cycling conditions were as following: 95°C for 15 minutes (1 cycle), 95°C for 15 seconds and 60°C for 1 minute (40 cycles). The threshold cycle (Ct) was calculated by the instrument's software (7500 Fast System SDS Software version 1.4). Analysis of the relative mRNA expression was performed using the ΔΔCt method. GAPDH mRNA was used for normalizing.

2.4 | Western blot analysis

Following stimulation, medium from the 6-well plates was aspirated completely and the cells were washed once with PBS solution. After adding 75 µL of cold lysis buffer (50 mM Tris-HCl, pH 7.4, 150 mM NaCl, 10% glycerol, 1% Triton X-100, 2 mM ethylenediaminetetraacetic acid (EDTA), 2 mM ethylene glycol-bis(β-aminoethyl ether)-N,N,N′,N′,-tetraacetic acid, 40 mM β-glycerophate, 50 mM sodium fluoride, 10 mg/mL leupeptin, 10 mg/mL pepstatin A, 1 mM phenylmethyl sulphonyl fluoride), the cells were scraped and homogenized by sonication for 5 minutes. These samples were then centrifuged for 15 minutes at 16 200 g and the supernatant was collected for protein determination using BCA assay. Cell lysates containing equal amounts of protein (25 µg) were separated on sodium dodecyl sulfate-polyacrylamide gel electrophoresis (10% acrylamide gel) and transferred on to a nitrocellulose membrane and further subjected to Western blot analysis. The antibodies used in this study include COX-2 antibody (sc-1747 (M19), Santa Cruz, Heidelberg, Germany) and β-actin antibody (A-2228, Sigma Aldrich, Steinheim, Germany).

2.5 | PRESTO-Tango assay

The PRESTO-Tango assay was performed according to Kroeze et al.[22] Briefly, HTLA cells (HEK293 stable cell line expressing a tTA-dependant luciferase reporter and a β-arrestin2-TEV fusion gene) were cultured in DMEM medium supplemented with 10% FCS, puromycin (2 µg/mL), hygromycin (100 µg/mL), and maintained in a humidified condition at 37°C in 5% CO_2. Cells were grown in P100 cell culture dishes coated with Poly-L-Lysine (50 µg/mL dissolved in PBS). At 50% confluency, cells were transfected with the S1PR2-Tango construct (a gift from Bryan Roth, Addgene plasmid #66497; http://n2t.net/addgene:66497; using Lipofectamine 2000 according to the manufacturer's protocol (Thermo Fisher Scientific, Darmstadt, Germany). After 24 hours, cells were transferred in the HTLA selection medium onto a poly-L-Lysine coated 24-well plate (Greiner Bio-one). Cells were allowed to adhere to the surface for 4 hours, then the complete medium is replaced with minimal medium and cells were starved for 12-16 hours. After starvation, the cells were stimulated with S1P d18:1 and S1P d20:1 in different concentrations for 16 hours as depicted in Figure 4C, D. Luciferase activity was measured according to the manufacturer's protocol using the Dual-Luciferase Reporter Assay System (E1910, Promega, Madison, USA) on the GloMax Discover System (Promega, Madison, USA). The luciferase luminescence units were normalized to protein values analyzed using Bradford protein assay.

2.6 | Transient transfection of CHO-K1 cells

Chinese hamster ovary (CHO) cells (CHO-K1) were cultured in DMEM/F-12 (1:1) complete medium in the humidified temperature of 37°C in 5% CO_2. When cells reached 70% confluency the CHO-K1 cells were transiently transfected with S1P receptor 2 ($S1P_2$)-GFP (kindly provided by Dr. Deron Herr, Expression Drug Designs, San Diego, USA).[23] For Transfection, Lipofectamine 2000 (Thermo Fisher Scientific, Darmstadt, Germany) was utilized following the manufacturer's instructions. Following transfection, cells were transferred to poly-L-lysine coated µ-slide 8 well plates (ibidi 80 824). The next day, cells were treated for 2 hours with S1P d18:1 and S1P d20:1, respectively, or with S1P d20:1 for 1 hours followed by S1P d18:1. Thereafter, cells were fixed with 4% formalin solution for 30 minutes, washed with PBS and stained with DAPI for 5 minutes, and finally stored in PBS. Images were acquired using LSM 510 Meta microscope equipped with a Plan-Apochromat 63/1.4 oil immersion objective (Carl Zeiss, Jena, Germany) as described before.[24] For the quantification of $S1P_2$ internalization, ImageJ software was used to measure the fluorescence ratio of the cytoplasm and the plasma membrane. These ratios were used for data analysis which was performed using GraphPad Prism (v5.01; GraphPad Software Inc, San Diego, CA, USA). The image quantification was performed in a blinded fashion.

2.7 | Liquid chromatography/tandem mass spectrometry analysis

Tissue samples were mixed with 200 µL of extraction buffer (citric acid 30 mM, disodium hydrogen phosphate 40 mM) and spiked with 20 µL of the internal standard mixture. Afterwards, four zirconium oxide grinding balls and 600 µL

of methanol:chloroform:HCL (15:83:2, v/v/v) were added. Samples were homogenized using a swing mill (Retsch, Haan, Germany, 25 Hz for 2.5 minutes). Samples were further processed as described for plasma previously.[25] For tissue levels in mice, 8-week-old, male, C57BL/6J mice were obtained from Charles River, Sulzfeld, Germany. Tissue samples from patients were provided by the University Cancer Center Frankfurt (UCT). Written consent was obtained from all patients and the study was approved by the Institutional Review Boards of the UCT and the Ethical Committee of the University Hospital Frankfurt (project-number: SNO-7-2019). Internal standard mixture consisted of sphingosine d18:1-d7, sphinganine d18:0-d7, S1P d18:1-d7. Reference substances (sphingosine d18:1, sphingosine d20:1, sphinganine d18:0, sphinganine d20:0, S1P d18:1 and S1P d20:1) were purchased from Avanti Polar Lipids (Alabaster, USA).

For the analysis of PGE_2, cell pellets were resuspended in 200 µL of PBS. Samples were spiked with isotopically labeled internal standard (PGE_2-d4), 100 µL of EDTA solution (0.15 M) and 600 µL ethyl acetate. Afterward, samples were vortexed and centrifuged at 20 000 g for 5 minutes. The organic phase was removed and the extraction was repeated with 600 µL ethyl acetate. The organic fractions were combined and evaporated at a temperature of 45°C under a gentle stream of nitrogen. The residues were reconstituted with 50 µL of acetonitrile/water/formic acid (20:80:0.0025, v/v/v) and transferred to glass vials. For calibration standards and quality control samples, 200 µL of PBS were spiked with standard working solutions and processed like the samples, starting from spiking the internal standard.

The LC-MS/MS analysis was carried out using an Agilent 1290 Infinity LC system (Agilent, Waldbronn, Germany) coupled with a hybrid triple quadrupole linear ion trap mass spectrometer QTRAP 6500+ (Sciex, Darmstadt, Germany) equipped with a Turbo-V-source operating in negative ESI mode. The chromatographic separation was carried out using a Synergi Hydro-RP column (150 × 2 mm, 4 µm particle size and 80 Å pore size; Phenomenex, Aschaffenburg, Germany). A gradient program was employed at a flow rate of 300 µL/min. Mobile phase A was water/formic acid (100:0.0025, v/v) and mobile phase B was acetonitrile/formic acid (100:0.0025, v/v). The analytes were separated under gradient conditions within 16 minutes. The injection volume was 10 µL. The gradient program started with 90% A for 1 minute, then mobile phase A was decreased to 60% within 1 minute, held for 1 minute, further decreased to 50% within 1 minute and held for 2 minutes. Within 2 minutes, mobile phase A was further decreased to 10% and held for 1 minute. Within 1 minute, the initial conditions were restored, and the column was reequilibrated for 6 minutes. Mass spectrometric parameters were set as follows: Ionspray voltage −4500 V, source temperature 500°C, curtain gas 40 psi, nebulizer gas 40 psi and Turbo heater gas 60 psi. Both quadrupoles were running at unit resolution.

For analysis and quantification, Analyst Software 1.6.3 and Multiquant Software 3.0.2 (both Sciex, Darmstadt, Germany) were used. The following precursor-to-product ion transition was used for the quantification of PGE_2: m/z 351.2 → m/z 315.0. The peak area of the analyte was corrected by the peak area of the corresponding internal standard. The calibration curve was constructed using linear regression with $1/x^2$ weighting. The coefficient of correlation was at least 0.99. Variations in accuracy were less than 15% over the whole range of calibration, except for the lowest limit of quantification, where a variation in accuracy of 20% was accepted.

2.8 | Statistical analysis

Statistical analysis was performed in GraphPad Prism (v5.01; GraphPad Software Inc, San Diego, CA, USA). Sphingolipid levels in mouse CNS and human glioblastoma were compared using repeated measures ANOVA. All other statistical analyses were performed using one-sided ANOVA *Post-hoc* comparisons were performed using Tukey multiple comparison tests. Differences with $P < .05$ were considered as statistically significant.

3 | RESULTS

3.1 | S1P d20:1 is present in the CNS of healthy mice and in human glioblastoma tissue

A potential physiological and pathophysiological function of sphingolipids with C20-LCBs requires the proof of their presence in vivo. In this regard, we attempted to confirm previously published concentrations of sphingolipids in the CNS. However, in contrast to previous attempts, we used LC-MS/MS with the appropriate reference substrates and quantitatively analyzed sphingolipids with C20-LCBs for the first time in human CNS tissue.

In the cortex, the spinal cord and the cerebellum of healthy adult male C57BL/6J mice we found that sphinganine d20:0, sphingosine d20:1, and S1P d20:1 were detectable (Figure 1A-C). Interestingly, in all regions investigated, concentrations of sphingolipids with C20-LCBs were clearly lower compared to their C18-LCB counterpart (Figure 1A-C), with ratios ranging from 1:5 to 1:100.

S1P d20:1 was significantly higher in the cerebellum as compared to the cortex (mean difference = 204.2 ng/mg, 95%CI = 261.2 to 147.6, P value < .0001) or the spinal cord (mean difference = 270.4 ng/mg, 95%CI = 199.0 to 341.8, P value < .0001). Similar loco-regional differences in the CNS could not be found for sphingosine d20:1 or sphinganine d20:0.

Additionally, we analyzed samples of human glioblastoma tissue, acquired directly after primary surgical resection

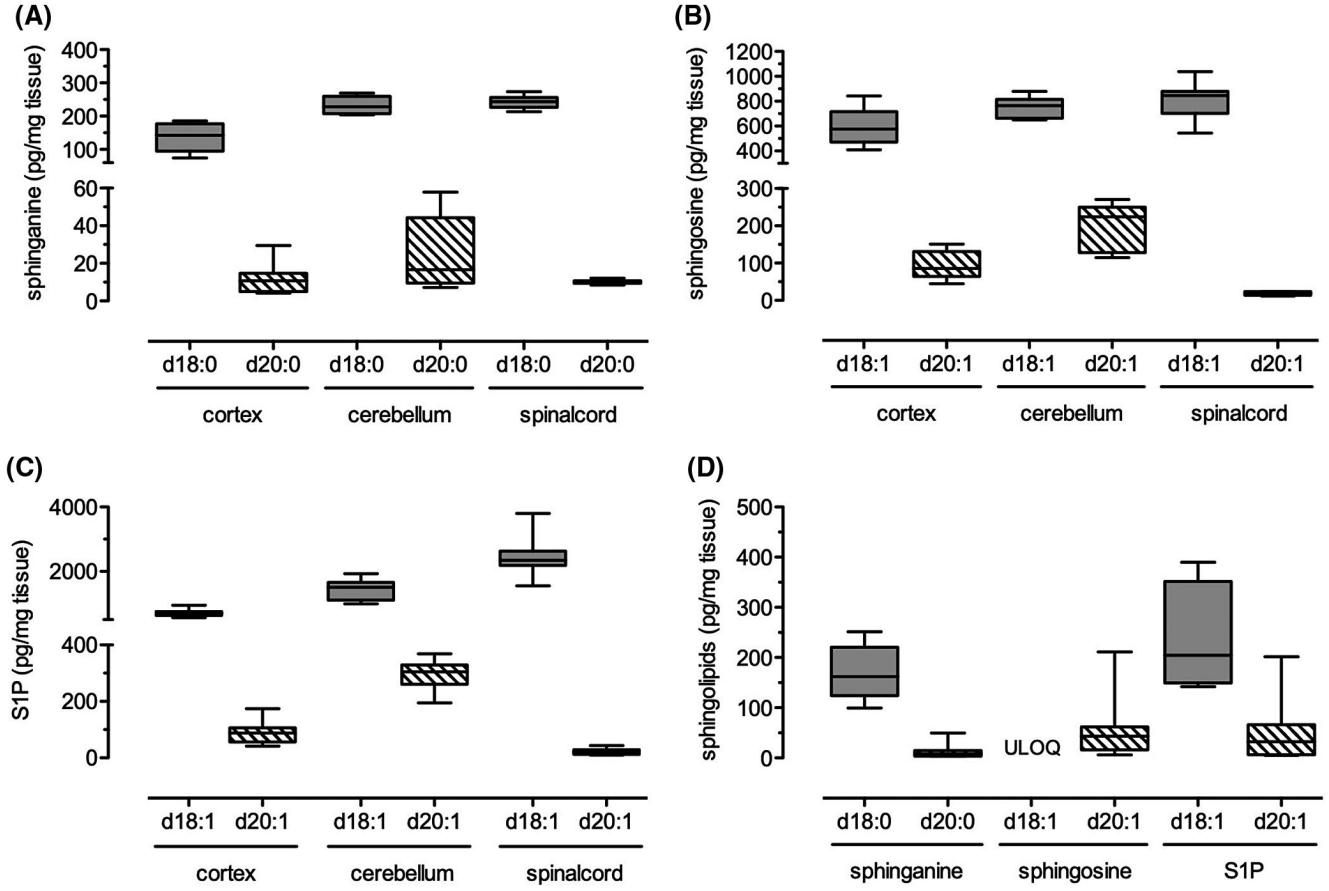

FIGURE 1 Presence of S1P d20:1 and its precursors in the CNS of mice and human glioblastoma samples. Sphingolipid levels were measured in mouse CNS tissue from male C57BL/6J mice (A-C) and human glioblastoma tissue (D) with LC-MS/MS as described in the Material and Methods section. Data are shown as boxplots with median values and the upper and lower quartile ± minimum and maximum values (n = 10; D: sphingosine: All samples over the upper limit of quantification (ULOQ) of 2500 pg/mg tissue)

(Figure 1D). First of all, sphinganine d20:0, sphingosine d20:1, and S1P d20:1 could be detected in GBM tissue. Of note, the concentrations varied considerably between patients (eg, S1P d20:1, min.: 5.2 ng/mg, max.: 201.5 ng/mg).

Interestingly, the S1P d18:1 level was considerably lower compared to healthy mouse tissue, while other sphingolipid levels measured were in a similar range (Figure 1).

3.2 | S1P d20:1 suppresses COX-2 upregulation induced by S1P d18:1 via $S1P_2$

To get indications for a potential pathophysiological relevance in glioblastoma, we investigated the capability of S1P d20:1 to induce COX-2 expression and activity in the LN229 glioblastoma cell line.

First of all, we replicated in glioblastoma cells the finding, previously published in renal mesangial cells,[5] that a stimulation with S1P d18:1 consistently induced COX-2 mRNA expression in a time and concentration-dependent manner (Figure 2A,B) as well as COX-2 protein expression (Figures 2F, 3B,E) and the formation of PGE_2 (Figure 3C). COX-1 expression was not influenced by either S1P d18:1 or S1P d20:1 (data not shown). The effect of S1P d18:1 on COX-2 mRNA (S1P d18:1 vs S1P d18:1 + JTE-013: Mean difference = 10.1 [fold expression relative to control], 95%CI = 8.6 to 11.7, P value < .001) and protein (S1P d18:1 vs S1P d18:1 + JTE-013: Mean difference = 2.6 [fold expression relative to control], 95%CI = 1.2 to 3.9, P value < .01) was blocked by 10 μM JTE-013, indicating the necessity of $S1P_2$ signaling pathways for COX-2 induction in this cell line (Figure 2E,F). Stimulation with 1 μM S1P d20:1 for 2 hours significantly induced the COX-2 mRNA but not COX-2 protein levels or the amount of PGE_2 (Figures 2C,D and 3B,C). Further analysis also revealed that lower doses of S1P d20:1 (0.01 μM and 0.1 μM) are sufficient to abate mRNA and protein expression of COX-2 induced by either 1 μM S1P d18:1 or 0.1 μM S1P d18:1 respectively (Figure 3D,E).

The lower efficacy of S1P d20:1 to induce COX-2 via $S1P_2$-mediated signaling could be the consequence of a much lower affinity of S1P d20:1 to bind to $S1P_2$, thus displaying only partial agonistic activity. In this case, co-stimulation of

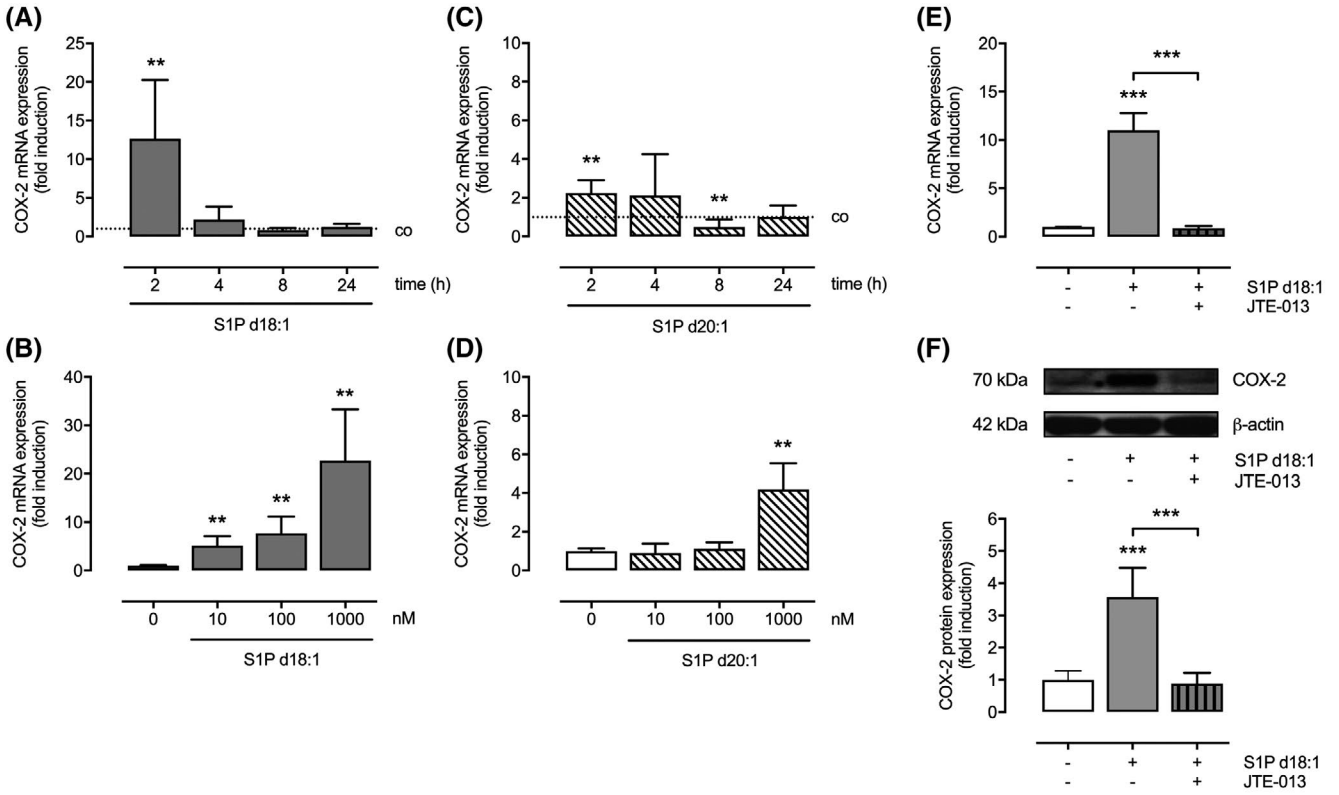

FIGURE 2 S1P d18:1-dependent COX-2 expression in LN229 cells is mediated via $S1P_2$. A-D: Time and concentration-dependent effect of S1P d18:1 and S1P d20:1 on COX-2 mRNA expression. Cells were stimulated with 1 μM S1P d18:1 and 1 μM S1P d20:1 for the indicated time points (A and C) or with the indicated concentrations for 2 hours (B and D). E-F: Effect of JTE-013 on S1P d18:1-dependent COX-2 mRNA (E) and protein expression (F) in LN229 cells. Cells were stimulated for 2 hours with 1 μM S1P d18:1 in the absence or presence of 10 μM JTE-013. COX-2 mRNA and protein expression was measured by TaqMan and Western blot analysis respectively as described in the Material and Methods section. All experiments were conducted as duplicates of three independent experiments. Data are shown as means ± SD.***$P < .001$ and **$P < .01$

cells with S1P d20:1 and S1P d18:1 might reduce the efficacy of S1P d18:1 on COX-2 induction. Indeed, we found here, that 1 μM of S1P d20:1 added to the same amount of S1P d18:1 led to lower levels of COX-2 mRNA (Figure 3A; S1P d18:1 vs S1P d18:1 + d20:1, mean difference = 9.4 [fold expression relative to control], 95% CI = 6.2 to 12.7, P value < .0001) compared to S1P d18:1 alone. Importantly, this effect could be confirmed by Western blot (Figure 3B; mean difference = 1.1 [fold expression relative to control], 95% CI = 0.14 to 2.2, P value < .05) and PGE_2 levels in the supernatant (Figure 3C; mean difference = 144.8 [ng/mg], 95% CI = 65.2 to 224.3, P value < .001).

3.3 | S1P d20:1 inhibits $S1P_2$ activation and internalization by S1P d18:1

As a consequence of our observation that S1P d20:1 inhibits S1P d18:1 and $S1P_2$-mediated COX-2 induction, we further tested the hypothesis that S1P d20:1 only partially activates $S1P_2$.

By using Chinese hamster ovary (CHO) cells, transfected with a $S1P_2$-GFP construct, we analyzed $S1P_2$ internalization in response to S1P. Here, we found that while S1P d18:1 lead to a strong internalization of $S1P_2$-GFP as expected, only a very limited internalization could be detected after stimulation with S1P d20:1. In the case of a co-stimulation with both, S1P d18:1 and d20:1, we found an intermediate localization of $S1P_2$-GFP signal with partial fluorescence localized to the membrane and some internalization of the $S1P_2$-GFP construct (Figure 4A). The GFP signal of the $S1P_2$ receptor was quantified in a blinded fashion using Image J software wherein the fluorescence ratio between the cytosol and plasma membrane were considered. The quantification co-related with the observed images, as the ratio of GFP signal in the cytoplasm was significantly higher in case of the treatment with 1 μM S1P d18:1 whereas highest plasma membrane signal was detected in S1P d20:1 treated cells followed by combination treatment of 1 μM S1P d20:1 and 1 μM S1P d18:1 (Figure 4B).

In order to verify and quantify this qualitative observation, we used a Presto-Tango assay with a $S1P_2$-TEV-TF

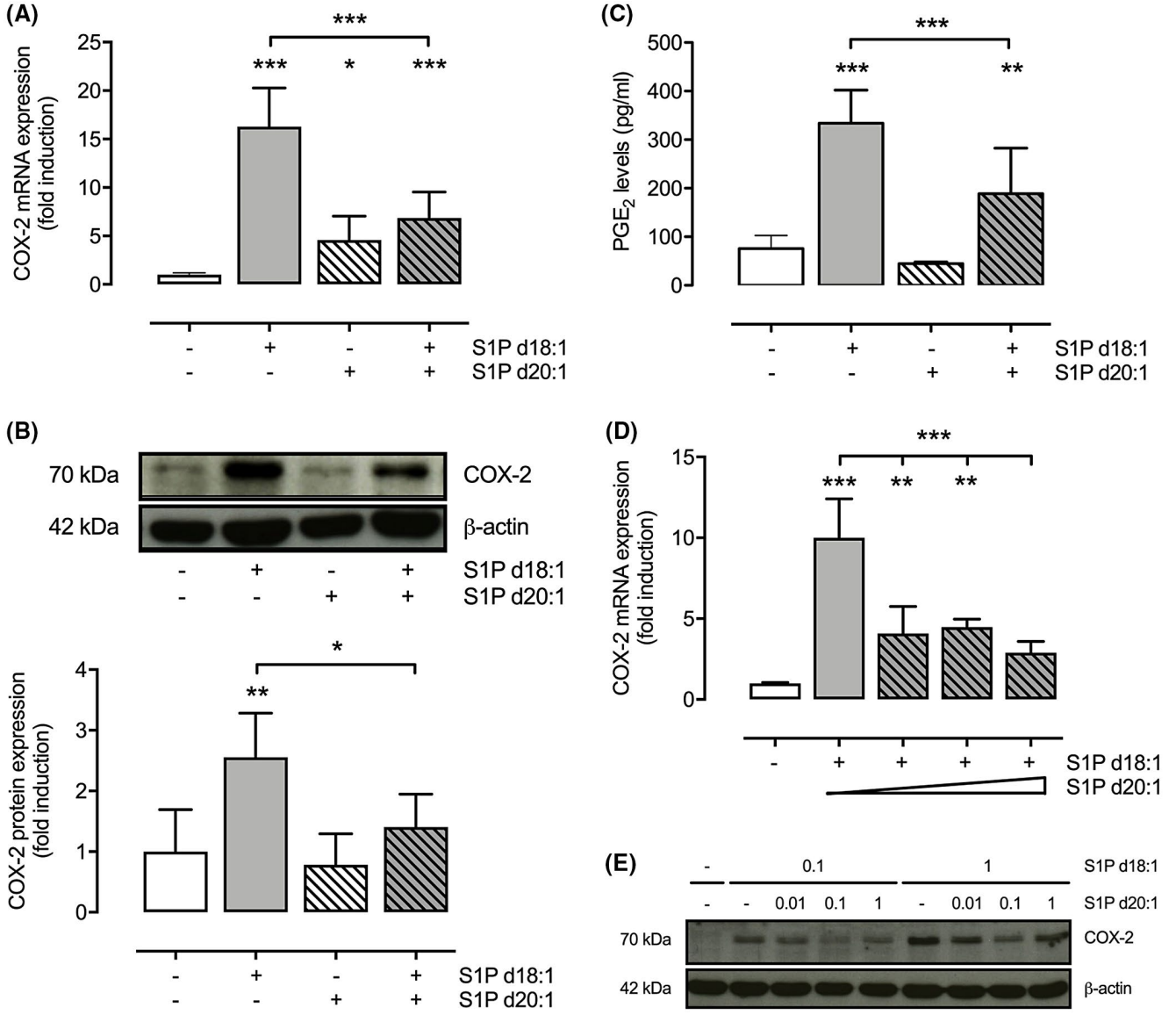

FIGURE 3 S1P d20:1 modulates S1P d18:1-dependent effect of COX-2 expression and the formation of PGE_2. A and B, Effect of S1P d20:1 on S1P d18:1-dependent COX-2 mRNA (A) and protein expression (B) in LN229 cells. Cells were stimulated for 2 hours with 1 μM S1P d18:1 and/or 1 μM S1P d20:1 as indicated. C, Quantification of PGE_2 levels in cell supernatant. Cells were stimulated for 2 hours with 1 μM S1P d18:1 and/or 1 μM S1P d20:1 as indicated. D, Concentration-dependent effect of S1P d20:1 on S1P d18:1-dependent COX-2 mRNA expression. Cells were stimulated for 2 hours with 1 μM S1P d18:1 and 0.01 μM, 0.1 μM and 1 μM S1P d20:1. E, Representative Western blot of the concentration-dependent effect of S1P d20:1 on S1P d18:1-dependent COX-2 protein expression. Cells were stimulated for 2 hours with either 0.1 μM or 1 μM S1P d18:1 and 0.01 μM, 0.1 μM, and 1 μM S1P d20:1. COX-2 mRNA and protein expression were measured by TaqMan and Western blot analysis respectively and PGE_2 levels were measured by LC-MS/MS as described in the Material and Methods section. All experiments were conducted as duplicates of three to five independent experiments. Data are shown as means ± SD. ***$P < .001$, **$P < .01$ and *$P < .05$

construct (Figure 4C,D). As shown in Figure 4C, we found an induction of Luciferase expression after stimulation with S1P d18:1 in comparison to control conditions (S1P d18:1 vs control: Mean difference = 1.3 [fold expression relative to control], 95%CI = 7.2 to 19.6, P value < .001) but not with d20:1 (S1P d20:1 vs control: Mean difference = 2.5 [fold expression relative to control], 95%CI = −59.8 to 64.7). In this case, no induction of Luciferase expression could be detected after a stimulation with S1P d18:1 plus d20:1 in comparison to control conditions (S1P d18:1 + S1P d20:1 vs control: Mean difference = 0.2 [fold expression relative to control], 95%CI = −0.4 to 0.8). Also, in Presto-Tango assay, we detected the concentration-dependent inhibitory effect of S1P d20:1 (0.01 μM – 1 μM) on $S1P_2$ receptor activation mediated by 1 μM S1P d18:1 (Figure 4D), indicating that low concentration of S1P d20:1, such as those documented by us

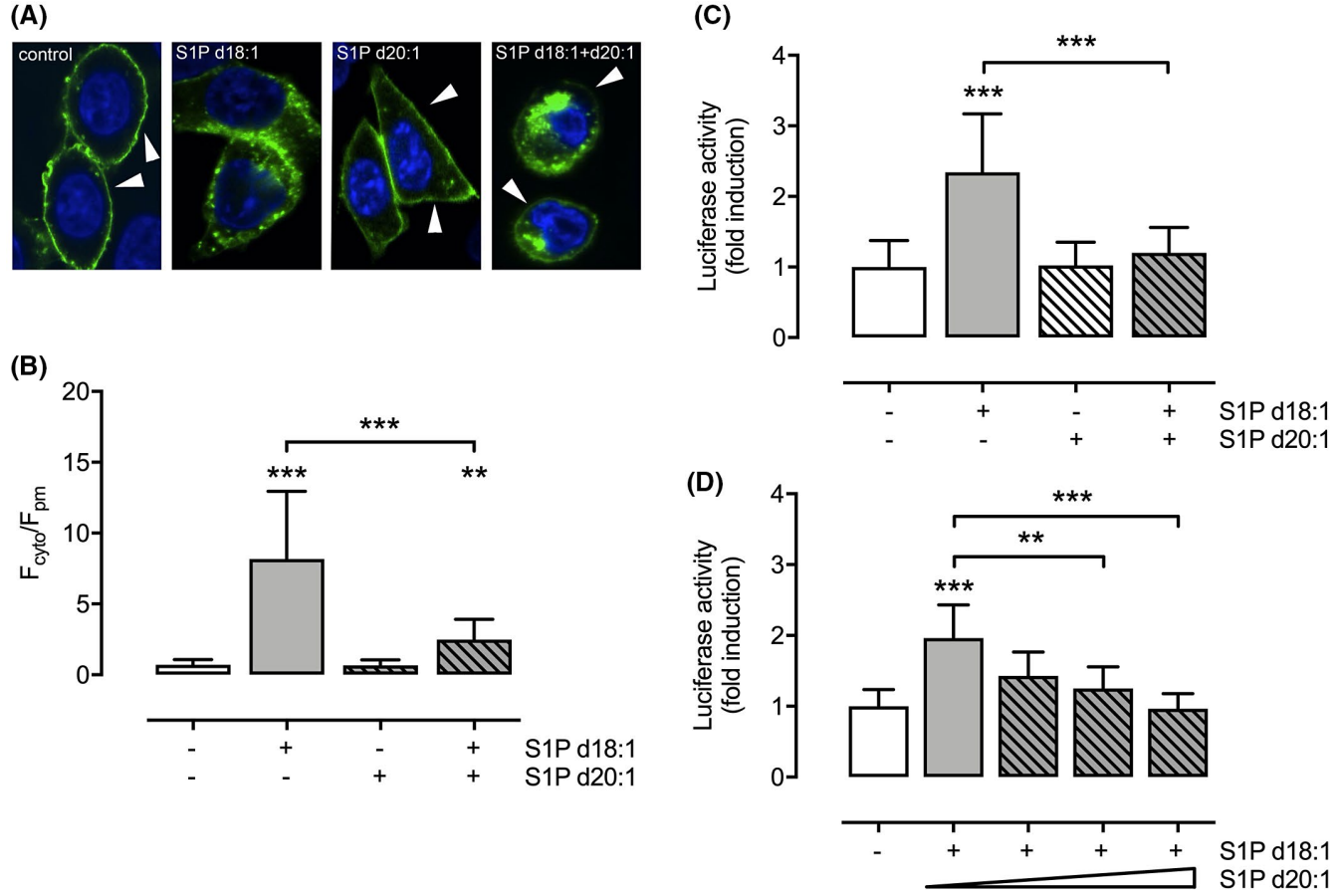

FIGURE 4 S1P d20:1 inhibits S1P d18:1-dependent activation of $S1P_2$. A, Representative images of CHO cells transfected with $S1P_2$-GFP and treated for 2 hours with either vehicle, 1 μM S1P d18:1 and 1 μM S1P d20:1 as indicated. Arrowheads indicate membrane localization. B, Quantification of A by analyzing the fluorescence ratio between cytosol and the plasma membrane of at least 14-15 fields in a μ-slide 8 well plate (four independent experiments). C and D, Luciferase activity induced by $S1P_2$ activation. Cells were treated for 16 hours with either vehicle, 1 μM S1P d18:1 and/or 1 μM S1P d20:1 (C) or with 1 μM S1P d18:1 and 0.01 μM, 0.1 μM and 1 μM S1P d20:1 (D). All experiments were conducted as duplicates of three to four independent experiments. Data in B are shown as means ± SD. $^{**}P < .05$ and $^{***}P < .001$

in the healthy CNS, are sufficient to block S1P d18:1-related $S1P_2$ activation further supporting our internalization data in CHO cells.

4 | DISCUSSION

In this study, we determined the concentrations of sphinganine d20:0, sphingosine d20:1, and S1P d20:1 in the healthy CNS of mice and in human glioblastoma tissue. On the functional level, we show that S1P d20:1 only moderately induces COX-2 at high concentrations. Importantly, S1P d20:1 is able to block S1P d18:1-mediated COX-2 induction. Concerning the mechanism, we show that S1P d20:1 has only a minimal activity of $S1P_2$ receptor activation and subsequent internalization. However, S1P d20:1 strongly reduced $S1P_2$ receptor activity upon S1P d18:1, thus arguing that S1P d20:1 acts as a partial agonist at the $S1P_2$ receptor.

Moreover, concentrations of sphingolipids with a C20-LCB are much lower compared to their C18 counterpart. This is in line with the observation that palmitoyl-CoA is the main substrate for the SPT.[26] Furthermore, the magnitude of C20-LCB concentrations and the relative relation to C18-LCBs we detected fit also well to the concentrations described in plasma by others[16,27] and to older data from the brain and spinal cord of the rabbit.[21]

However, to our surprise, our data in part disagree with the most recent two publications of C20-LCB concentrations in the CNS.[17,19] Most recently, Zhao et al[17] described levels of S1P d20:1 and sphingosine d20:1 at least as high as S1P d18:1 and sphingosine d18:1 in the CNS of mice. Their data is in part supported by the observation that gangliosides in the CNS with sphingosine d20:1 in the rat and human brain represent 50% of ganglioside LCBs in the adult.[19] However, Sonnino et al[19] provide data about the concentration of the LCBs of all sphingolipids, and thus are not able to postulate

assumptions about the concentration of free sphinganine d20:0 or sphingosine d20:1. Interestingly, this might indicate that S1P d20:1 and sphingosine d20:1 are directly generated by the sphingolipid de novo synthesis pathway and not by hydrolysis of complex sphingolipids such as gangliosides. This is in line with previous observations that the treatment of cells with [^{14}C]stearic acid leads to a higher content of C20-LCB gangliosides but not of sphingosine d20:1.[28]

In general, the most likely explanation for the detection of different levels with C20-LCBs in comparison to Zhao et al[17] is the use of divergent analytical methods. While we used LC-MS/MS with S1P d20:1 as a reference substrate and S1P d18:1 as the deuterated standard, Zhao et al used the calibration curves of C18-LCBs for C20-LCB quantification. As a limitation of both studies, the most accurate methodology to quantify the S1P d20:1 level would be the comparison with a deuterated S1P d20:1 standard, which, however, is not available so far.

COX-2 induction by S1P is a well-known cellular response that is described in various cell types and tissues.[5-7,29,30] Most of the current data to date points to a $S1P_2$-mediated mechanism,[5,6] however, tissue/cell-specific mechanisms are likely.[30] We show the importance of $S1P_2$ signaling for COX-2 induction in the glioma cell line LN229 by the use of JTE-013 an extensively characterized inhibitor of $S1P_2$. This is well in line with the frequent observation that, depending on the cell type, $S1P_2$ mediates the proinflammatory actions of S1P.[31] Importantly, S1P has been shown to be upregulated in glioblastoma while the sphingosine kinase 1-$S1P_2$ axis mediates glioma cell migration.[32] Moreover, COX-2 has been shown to be involved in the pathophysiology of glioblastoma.[33] Thus, it is tempting to speculate that the dose-dependent induction of COX-2 by S1P d18:1 might contribute to glioma invasiveness.

Importantly, our observation that a co-stimulation with S1P d18:1 and d20:1 leads to reduced COX-2 mRNA levels indicates a partial agonism of S1P d20:1 at the $S1P_2$ receptor. The effects on COX-2 protein, PGE_2 levels and results from the Presto-Tango assays may even be interpreted as pure antagonistic function. Thus, moreover, S1P d20:1 must have an at least similar affinity to the $S1P_2$ receptor, but a lower efficacy. This assumption is partly in line with the hypothesis that the S1P head group determines the binding affinity, while the alkyl chain drives receptor activation.[34] However, these results are contradictive to a recent report that S1P d20:1 has a lower potency but higher efficacy at $S1P_2$ compared to S1P d18:1.[18] This discrepancy is to some degree explainable by different concentrations applied, that is, the higher efficacy of S1P d20:1 demonstrated by Troupiotis-Tsaïlaki et al[18] was shown only at concentrations above 1 μM.

While we used this experimental setup primarily as a proof of principle, our finding that S1P- d20:1 inhibits S1P d18:1-$S1P_2$-mediated signaling might suggest that potential S1P d18:1-induced proinflammatory and angiogenic mechanisms in glioblastoma can be modulated by S1P d20:1. It will be interesting to see whether the regulation of S1P d20:1 level modulates features of glioblastoma biology such as invasiveness, proliferation, and angiogenesis, both features known to be influenced by $S1P_2$ signaling.[35]

Furthermore, S1P d20:1 could also inhibit $S1P_2$-mediated proinflammatory signals in other pathologies, such as those mediating blood-brain barrier permeability.[36] In this line, S1P d20:1 could reduce $S1P_2$-mediated blood-brain barrier disruption in pathologies such as stroke[37] or multiple sclerosis.[38]

Intriguingly, concentrations of S1P measured in organisms are often much higher than the K_d values of their receptors (eg, $S1P_2$ K_d = 16-27 nM[39]). This is indicative of complex regulation of S1P signaling in vivo. Known regulative mechanisms are the relative S1P receptor subtype expression, their localization, as well as the local activity of S1P metabolizing lyases and phosphatases. Due to its action as a partial receptor agonist that we observed in this study, we propose that the S1P d20:1 level is another important endogenous mechanism to keep S1P signaling in check. In addition, we could also show that S1P d20:1 even at low concentrations could inhibit both, COX-2 mRNA and protein expression upregulated by S1P d18:1 in LN229 as well as inhibit $S1P_2$ receptor activation in CHO cells and PRESTO-Tango assay. Even in vivo, there exist low concentrations of S1P d20:1 compared to very high levels of S1P d18:1 and our data strengthen the relevance of S1P d20:1 at such low concentrations. Thus, in the future, it is crucial to investigate how the organism controls the local S1P d20:1 concentration and the mechanism of inhibition of S1P d18:1-mediated $S1P_2$ activation. Targeting the responsible enzymes could represent yet another potential therapeutic approach in modulating S1P signaling in diseases.

In conclusion, we provide a new mechanism of S1P receptor signaling. With achieving our main goal to demonstrate the concept of S1P d20:1-mediated modulation of S1P signaling, further questions need to be addressed in future studies. Our data suggest that the consideration of the S1P d20:1 level is necessary to understand the cell biological effects of S1P d18:1 in vivo. Further research regarding the metabolism of S1P d20:1 is warranted.

ACKNOWLEDGMENTS

This work was supported by the German Research Foundation (SFB 1039 to RB, WP, JP, DMzH), and the Foundation Leducq (to WP and JP).

CONFLICT OF INTEREST

The authors declare no conflict of interest.

AUTHOR CONTRIBUTIONS

RV, AK, and FM designed and conducted experiments. RB, WP, JP, DMzH, and AK designed experiments and wrote manuscripts. ST, YS, and DT performed mass spectrometry.

REFERENCES

1. Hannun YA, Obeid LM. Sphingolipids and their metabolism in physiology and disease. *Nat Rev Mol Cell Biol* [Internet]. 2018 Mar 22 [cited 2019 Jul 24];19(3):175-191. http://www.nature.com/articles/nrm.2017.107.
2. Proia RL, Hla T. Emerging biology of sphingosine-1-phosphate: its role in pathogenesis and therapy. *J Clin Invest* [Internet]. 2015 Apr 1 [cited 2019 Jul 24];125(4):1379-1387. http://www.ncbi.nlm.nih.gov/pubmed/25831442.
3. Lee MJ, Thangada S, Claffey KP, et al. Vascular endothelial cell adherens junction assembly and morphogenesis induced by sphingosine-1-phosphate. *Cell* [Internet]. 1999 Oct 29 [cited 2019 Jul 24];99(3):301-312. http://www.ncbi.nlm.nih.gov/pubmed/10555146.
4. Garcia JGN, Liu F, Verin AD, et al. Sphingosine 1-phosphate promotes endothelial cell barrier integrity by Edg-dependent cytoskeletal rearrangement. *J Clin Invest* [Internet]. 2001 Sep 1 [cited 2019 Jul 24];108(5):689-701. http://www.ncbi.nlm.nih.gov/pubmed/11544274.
5. Völzke A, Koch A, Meyer zu Heringdorf D, et al. Sphingosine 1-phosphate (S1P) induces COX-2 expression and PGE2 formation via S1P receptor 2 in renal mesangial cells. *Biochim Biophys Acta - Mol Cell Biol Lipids* [Internet]. 2014 Jan [cited 2019 Jul 24];1841(1):11-21. http://www.ncbi.nlm.nih.gov/pubmed/24064301.
6. Skoura A, Michaud J, Im D-S, et al. Sphingosine-1-phosphate receptor-2 function in myeloid cells regulates vascular inflammation and atherosclerosis. *Arterioscler Thromb Vasc Biol* [Internet]. 2011 Jan [cited 2014 Sep 27];31(1):81-85. http://www.pubmedcentral.nih.gov/articlerender.fcgi?artxml:id=3013369&tool=pmcentrez&rendertype=abstract.
7. Sung HK, Min JC, Chang HL, Sang GK. Gα12 specifically regulates COX-2 induction by sphingosine 1-phosphate: role for JNK-dependent ubiquitination and degradation of IκBα. *J Biol Chem*. 2007 Jan 19;282(3):1938-1947.
8. Han G, Gupta SD, Gable K, et al. Identification of small subunits of mammalian serine palmitoyltransferase that confer distinct acyl-CoA substrate specificities. *Proc Natl Acad Sci* [Internet]. 2009 May 19 [cited 2019 Jul 24];106(20):8186-8191 http://www.ncbi.nlm.nih.gov/pubmed/19416851.
9. Hornemann T, Wei Y, von Eckardstein A. Is the mammalian serine palmitoyltransferase a high-molecular-mass complex? *Biochem J* [Internet]. 2007 Jul 1 [cited 2019 Jul 24];405(1):157-164. http://www.biochemj.org/cgi/doi/10.1042/BJ20070025.
10. Cowart LA, Hannun YA. Selective substrate supply in the regulation of yeast de novo sphingolipid synthesis. *J Biol Chem* [Internet]. 2007 Apr 20 [cited 2019 Jul 24];282(16):12330-12340. http://www.jbc.org/lookup/doi/10.1074/jbc.M700685200.
11. Mann N, Turner A, Sinclair A, Kelly F, Li D, Abedin L. A stearic acid-rich diet improves thrombogenic and atherogenic risk factor profiles in healthy males. *Eur J Clin Nutr*. 2002;55:88-96.
12. Kühn T, Floegel A, Sookthai D, et al. Higher plasma levels of lysophosphatidylcholine 18:0 are related to a lower risk of common cancers in a prospective metabolomics study. *BMC Med* [Internet]. 2016 Dec 28 [cited 2019 Jul 24];14(1):13. http://www.biomedcentral.com/1741-7015/14/13.
13. Mondul AM, Moore SC, Weinstein SJ, Karoly ED, Sampson JN, Albanes D. Metabolomic analysis of prostate cancer risk in a prospective cohort: the alpha-tocopherol, beta-carotene cancer prevention (ATBC) study. *Int J Cancer* [Internet]. 2015 Nov 1 [cited 2019 Jul 24];137(9):2124-2132. http://www.ncbi.nlm.nih.gov/pubmed/25904191.
14. Cross AJ, Moore SC, Boca S, et al. A prospective study of serum metabolites and colorectal cancer risk. *Cancer* [Internet]. 2014 Oct 1 [cited 2019 Jul 24];120(19):3049-3057. http://www.ncbi.nlm.nih.gov/pubmed/24894841.
15. Chajès V, Hultén K, Van Kappel AL, et al. Fatty-acid composition in serum phospholipids and risk of breast cancer: an incident case-control study in Sweden. *Int J Cancer* [Internet]. 1999 Nov 26 [cited 2019 Jul 24];83(5):585-590. http://doi.wiley.com/10.1002/%28SICI%291097-0215%2819991126%2983%3A5%3C585%3A%3AAID-IJC2%3E3.0.CO%3B2-Z.
16. Othman A, Saely CH, Muendlein A, et al. Plasma C20-Sphingolipids predict cardiovascular events independently from conventional cardiovascular risk factors in patients undergoing coronary angiography. *Atherosclerosis* [Internet]. 2015 May [cited 2018 Sep 16];240(1):216-221. http://linkinghub.elsevier.com/retrieve/pii/S0021915015001719.
17. Zhao L, Spassieva S, Gable K, et al. Elevation of 20-carbon long chain bases due to a mutation in serine palmitoyltransferase small subunit b results in neurodegeneration. *Proc Natl Acad Sci* [Internet]. 2015;112(42):12962-12967. http://www.pnas.org/lookup/doi/10.1073/pnas.1516733112.
18. Troupiotis-Tsaïlaki A, Zachmann J, González-Gil I, et al. Ligand chain length drives activation of lipid G protein-coupled receptors. *Sci Rep* [Internet]. 2017 Dec 17 [cited 2019 Jul 24];7(1):2020. http://www.nature.com/articles/s41598-017-02104-5.
19. Sonnino S, Chigorno V. Ganglioside molecular species containing C18- and C20-sphingosine in mammalian nervous tissues and neuronal cell cultures. *Biochim Biophys Acta—Rev Biomembr* [Internet]. 2000 Sep [cited 2019 Jul 24];1469(2):63-77. https://linkinghub.elsevier.com/retrieve/pii/S0005273600002108.
20. Sambasivarao K, McCluer RH. Lipid components of gangliosides. *J Lipid Res* [Internet]. 1964 Jan [cited 2019 Jul 24];15:103-108. http://www.ncbi.nlm.nih.gov/pubmed/14173314.
21. Schwarz HP, Kostyk I, Marmolejo A, Sarappa C. Long-chain bases of brain and spinal cord of rabbits. *J Neurochem* [Internet]. 1967 Jan [cited 2019 Jul 24];14(1):91-97. http://www.ncbi.nlm.nih.gov/pubmed/6018082.
22. Kroeze WK, Sassano MF, Huang X-P, et al. PRESTO-Tango as an open-source resource for interrogation of the druggable human GPCRome. *Nat Struct Mol Biol* [Internet]. 2015 May 20 [cited 2019 Sep 1];22(5):362-369. http://www.ncbi.nlm.nih.gov/pubmed/25895059.
23. Harris GL, Creason MB, Brulte GB, Herr DR. In vitro and in vivo antagonism of a G protein-coupled receptor (S1P3) with a novel blocking monoclonal antibody. *PLoS ONE* [Internet]. 2012 Apr 5 [cited 2019 Sep 16];7(4):e35129. http://www.ncbi.nlm.nih.gov/pubmed/22496900.
24. Imeri F, Fallegger D, Zivkovic A, et al. Novel oxazolo-oxazole derivatives of FTY720 reduce endothelial cell permeability, immune cell chemotaxis and symptoms of experimental autoimmune encephalomyelitis in mice. *Neuropharmacology* [Internet]. 2014 Oct

[cited 2019 Sep 16];85:314-327. https://linkinghub.elsevier.com/retrieve/pii/S0028390814001798.
25. Brunkhorst R, Pfeilschifter W, Patyna S, et al. Preanalytical biases in the measurement of human blood sphingolipids. *Int J Mol Sci*. 2018;19(5):1390.
26. Hornemann T, Penno A, Rütti MF, et al. The SPTLC3 subunit of serine palmitoyltransferase generates short chain sphingoid bases. *J Biol Chem* [Internet]. 2009 Sep 25 [cited 2019 Aug 23];284(39):26322-26330. http://www.ncbi.nlm.nih.gov/pubmed/19648650.
27. Suriyanarayanan S, Othman A, Dräger B, et al. A novel variant (Asn177Asp) in SPTLC2 causing hereditary sensory autonomic neuropathy type 1C. *NeuroMolecular Med* [Internet]. 2019 Jun 6 [cited 2019 Aug 22];21(2):182-191. http://www.ncbi.nlm.nih.gov/pubmed/30955194.
28. Chigorno V, Valsecchi M, Sonnino S. Biosynthesis of gangliosides containing C18:1 and C20:1 [3-14C]sphingosine after administrating [1-14C]palmitic acid and [1-14C]stearic acid to rat cerebellar granule cells in culture. *Eur J Biochem* [Internet]. 1994 May 1 [cited 2019 Jul 4];221(3):1095-1101. http://www.ncbi.nlm.nih.gov/pubmed/8181467.
29. Hsu C-K, Lee I-T, Lin C-C, Hsiao L-D, Yang C-M. Sphingosine-1-phosphate mediates COX-2 expression and PGE2 /IL-6 secretion via c-Src-dependent AP-1 activation. *J Cell Physiol* [Internet]. 2015;230(3):702-715. http://www.ncbi.nlm.nih.gov/pubmed/25201048.
30. Kim JI, Jo EJ, Lee H-Y, et al. Sphingosine 1-phosphate in amniotic fluid modulates cyclooxygenase-2 expression in human amnion-derived WISH cells. *J Biol Chem* [Internet]. 2003 Aug 22 [cited 2019 Aug 23];278(34):31731-31736. http://www.ncbi.nlm.nih.gov/pubmed/12796504.
31. Blankenbach KV, Schwalm S, Pfeilschifter J, Meyer zu Heringdorf D. Sphingosine-1-phosphate receptor-2 antagonists: therapeutic potential and potential risks. *Front Pharmacol* [Internet]. 2016 [cited 2019 Jun 25];7(JUN). www.frontiersin.org.
32. Mahajan-Thakur S, Bien-Möller S, Marx S, Schroeder H, Rauch BH. Sphingosine 1-phosphate (S1P) signaling in glioblastoma multiforme—a systematic review. *Int J Mol Sci* [Internet]. 2017 Nov 17 [cited 2019 Aug 12];18(11). http://www.ncbi.nlm.nih.gov/pubmed/29149079.
33. Qiu J, Shi Z, Jiang J. Cyclooxygenase-2 in glioblastoma multiforme. *Drug Discov Today* [Internet]. 2017 Jan [cited 2019 Aug 22];22(1):148-156. http://www.ncbi.nlm.nih.gov/pubmed/27693715.
34. O'Sullivan C, Dev KK. The structure and function of the S1P1 receptor. *Trends Pharmacol Sci* [Internet]. 2013 Jul 1 [cited 2019 Aug 23];34(7):401-412. https://linkinghub.elsevier.com/retrieve/pii/S0165614713000801.
35. Lepley D, Paik J-H, Hla T, Ferrer F. The G protein-coupled receptor S1P2 regulates Rho/Rho kinase pathway to inhibit tumor cell migration. *Cancer Res* [Internet]. 2005 May 1 [cited 2014 Aug 1];65(9):3788-3795. http://www.ncbi.nlm.nih.gov/pubmed/15867375.
36. Sanchez T, Skoura A, Wu MT, Casserly B, Harrington EO, Hla T. Induction of vascular permeability by the sphingosine-1-phosphate receptor–2 (S1P2R) and its downstream effectors ROCK and PTEN. *Arterioscler Thromb Vasc Biol* [Internet]. 2007 Jun [cited 2019 Aug 22];27(6):1312-1318. http://www.ncbi.nlm.nih.gov/pubmed/17431187.
37. Kim GS, Yang L, Zhang G, et al. Critical role of sphingosine-1-phosphate receptor-2 in the disruption of cerebrovascular integrity in experimental stroke. *Nat Commun* [Internet]. 2015 Nov 5 [cited 2019 Aug 23];6(1):7893. http://www.nature.com/articles/ncomms8893.
38. Cruz-Orengo L, Daniels BP, Dorsey D, et al. Enhanced sphingosine-1-phosphate receptor 2 expression underlies female CNS autoimmunity susceptibility. *J Clin Invest* [Internet]. 2014 Jun [cited 2019 Aug 23];124(6):2571-2584. http://www.ncbi.nlm.nih.gov/pubmed/24812668.
39. Ancellin N, Differential HT. Pharmacological properties and signal transduction of the sphingosine 1-phosphate receptors EDG-1, EDG-3, and EDG-5. *J Biol Chem* [Internet]. 1999 Jul 2 [cited 2019 Aug 20];274(27):18997-19002. http://www.jbc.org/lookup/doi/10.1074/jbc.274.27.18997.

How to cite this article: Vutukuri R, Koch A, Trautmann S, et al. S1P d20:1, an endogenous modulator of S1P d18:1/S1P$_2$-dependent signaling. *The FASEB Journal*. 2020;34:3932–3942. https://doi.org/10.1096/fj.201902391R